Discrimination of Closely-Spaced Geosynchronous Satellites – Phase Curve Analysis & New Small Business Innovative Research (SBIR) Efforts

Paul LeVan
Air Force Research Laboratory
Space Vehicles Directorate
Kirtland Air Force Base, NM 87117-5776

ABSTRACT

Geosynchronous objects appear as unresolved blurs even when observed with the largest ground-based telescopes. Due to the lack of any spatial detail, two or more objects appearing at similar brightness levels within the spectral bandpass they are observed are difficult to distinguish. Observing a changing pattern of such objects from one time epoch to another showcases the deficiencies in associating individual objects before and after the configuration change. This paper explores solutions to this deficiency in the form of spectral (under small business innovative research) and phase curve analyses. The extension of the technique to phase curves proves to be a powerful new capability.

1. INTRODUCTION

Recent AMOS Technical Conference papers (e.g., [1]) have emphasized examples of multiple satellites occupying the same geosynchronous slot, with individual satellites maneuvering about one another in intricate ways. These examples have been shown to result in configurations where the individual objects appear to "coalesce" along the observational line of sight, effectively resulting in one mega-object on the scale of the seeing-limited resolution of ground-based observations and pixel fields of view. In this situation, maintenance of the individual tracks is precluded over the course of the conjunction and re-identification of the objects thereafter is problematic. A recent SBIR topic (AF093-056) seeks innovation in the area of improved spectral discrimination of closely-spaced geosynchronous satellites, with GEODSS (Ground-based Electro-Optical Deep Space Surveillance) and related ground-based observing systems as the identified application.

Spectral techniques have been shown useful in providing a means of discrimination. In one scenario, objects differentiated by their spectral shape prior to merging can be re-identified once they again become spatially distinct. As a more stressing example, objects that have been maneuvered into an un-resolvable configuration still provide a "composite" spectrum that is typically the sum of their individual spectra. The observation of the predicted shape of the composite spectrum would serve to account for the individual objects while in the spatially-unresolved configuration.

The challenges for solutions proposed for this SBIR topic lay in the demonstration of needed levels of signal-to-noise ratio over times likely to be allocated to spectral observations in a dedicated metric tracking facility. There is also the issue of compatibility of an approach with the existing facility sensor package, and ease of interpretation of the data product. However, the payoffs for a clever concept that is able to respond to these challenges would be a marked increase in ability to address the closely-spaced satellite issue.

Of the four contracts awarded under the SBIR, two are spectral in nature and employ dispersive elements, whereas two others are multi-band with spectral filter segregation on or near the sensor array.

2. OBSERVATIONAL CONSIDERATIONS

The relatively large distances to geosynchronous objects pose well-known limitations on spatial extent that even the largest ground-based telescope can resolve. Relatively good atmospheric seeing (in the range of one second of arc) translates to ~200 m at geosynchronous altitudes; satellites separated by this amount and

less, projected perpendicular to the line-of-sight, cannot be resolved. These are the limits against which many space surveillance network (SSN) assets without adaptive optics must work. It is for these reasons that alternative discrimination techniques are needed for geosynchronous clusters where multiple objects are located in one slot and experiencing relative motion as part of their station keeping (see, e.g., the Anik F1 & Anik F1-R example described in [1]).

Two techniques suggest themselves to enhance closely-space object (CSO) discrimination capabilities. One exploits differences in satellite spectral shapes; this has been described in [2] ("Paper I" hereafter) and related approaches are the subject of current SBIR efforts. Another attractive technique exploits phase curve differences among satellites; these have been described in impressive detail by Payne and co-workers ([3] & also prior AMOS Conference proceedings), *in the context of individual objects as opposed to clusters of unresolved satellites.* However, the techniques have an extension to the CSO discrimination problem, as will be described here.

In Paper I, *generalized radiometric signals* were described; these can range from simple brightness values in different wavebands to multiplicative combinations of the signals observed at different wavelengths that emphasize spectral slope or curvature. The key distinction is in the way that ratios of these generalized signals are formed among different satellites. The ratios are independent of sensor calibration and atmospheric transmission, as can be seen for the simple ratio $r_{ij} = s_i / s_j$, when the signals s for objects i and j have been observed along similar lines-of-sight over similar times. For the mathematical group approach of Paper I, it's helpful that $r_{ij} = 1/r_{ji}$ (i.e., exchanging the object ordering results in a reciprocal of the observed ratio); this is easily seen for the simple signal ratio given above and also applies for other more general forms of signal, e.g., *curvature*, defined for a single object as $(S_{\lambda 1} * S_{\lambda 3}) / S_{\lambda 2}^2$, where three signal values are measured at three wavelengths $\lambda 3 > \lambda 2 > \lambda 1$. When ratios of these generalized signals are plotted for multiple objects as have traditional color ratios been plotted over the years, a specific configuration of objects appears in a distinct area of the plot, and Paper I showed a means of interpreting changes in before-and-after positions on the plot along the lines of mathematical groups. For example, accounting for the change in configuration of three objects by associating each of the 36 possibilities in before and after ratio plots was shown possible in terms of S3 permutations.

Here we extend this line of attack from spectral to phase curve observations. As is the case for spectral observations, a large number of phase curve samples is not necessarily required; observations at several separated values of phase angle will often suffice. We take as examples data read visually from phase curves published for two objects, ANIK F1 and GOES 10, by Payne and co-workers[3]. The third object (labeled "synthetic" in Table 1) is an average of the first two objects' phase curves, with the GOES 10 curve scaled by the factor of 20 needed to match the overall level of the ANIK F1curve in a least-squares minimization. (The analysis that follows is independent of this scaling, which results in objects of similar brightness at a given phase angle, which would be difficult to distinguish by brightness alone.) It's also of no real consequence that the values are approximate as they only serve to illustrate the approach. For this scenario, let us imagine that phase curves are to be measured for three objects that are part of a cluster and individually resolvable. We make three sets of observations on the cluster satellites at three (somewhat arbitrary) phase angles: 0, 30, and 40 degrees. These signal levels, scaled relative to an $m_v = 14$ star, are presented in Table 1 and plotted in Fig. 1. The curvature signal described above in the context of spectra and applied here to phase curves is included in the last column of Table 1.

Table 1. Representative phase curve signals sampled at three discrete phase angles

Object	0^o	30^o	40^o	$S_0^o * S_{40}^o / (S_{30}^o)^2$
1 (ANIK F1)	100	42	50	2.8
2 (GOES 10)	5.2	2.5	1.7	1.4
3 (Synthetic)	102	46	42	2.0

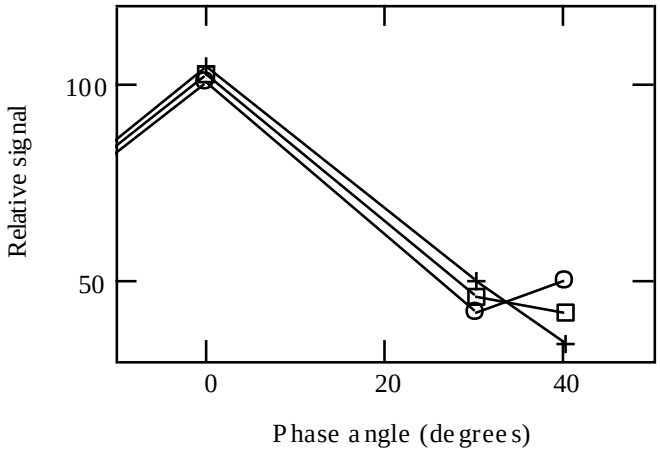

Fig. 1. Phase curve samples form Table 1, with GOES 10 (+ symbol) scaled by x20. (Lines connecting points are not representative of phase curve data between points; see [4] for the exquisite object information derivable with a fully-sampled phase curve.)

These objects are numbered 1 to 3 by an adopted convention that is respected for all epochs of data collection. Let us assume, for example, that the rankings of the Table 1 objects are by increasing longitude and then latitude for a given bin of longitude. Our observations will be plotted as signal ratios among the three objects, similar to color ratios in B-V-R photometry, for example. In this case the observations are independent of atmospheric transmission changes, and also independent of sensor gain calibration, requiring only that the gain be constant over the course of the observations.

Ordered pairs of ratios corresponding to all six possible object configurations are shown in Table 2 and plotted in Fig. 2, below, where the ratio pairs corresponding to the configuration of Table 1 (Anik F1, GOES 10, and "synthetic" ordered 1, 2, and 3) is circled. The observations are numbered moving clockwise away from the "identity configuration", and the associated ratios are listed in Table 2, where each ratio has been "decomposed" into the two signals that comprise it, to illustrate the exchange of objects. In practice, it is only the ratio of signals (a single number rather than a numerator and denominator that is shown in Table 2) that suffices for this suggested interpretation of phase curve data.

Table 2. Ratio pairs decomposed into numerator and denominator signal values to provide an appreciation for the effects of permutation. The numbering corresponds to that of Fig. 2 points.

Figure 2 Point	Object2 / Object1 ratio	Object3 / Object1 ratio	S3 permutation
1	1.4/2.8	2/2.8	identity
2	1.4/2	2.8/2	(13)
3	2/1.4	2.8/1.4	(231)
4	2.8/1.4	2.0/1.4	(12)
5	2.8/2	1.4/2	(312)
6	2/2.8	1.4/2.8	(23)

First, we note good separation of the objects in Fig. 2, based on the ratios of the selected "curvature" signal (suggesting that objects with somewhat similar phase curves could be distinguished with the technique, if the signal to noise ratio is reasonable). So far, what we have illustrated is an "interpretable" scheme for displaying phase curve data observed at a few discrete angles, which would permit observation of a larger number of objects over the course of a night by a single SSN asset. A change in configuration will be

indicated on the basis of the data points shown in Fig. 2 that are subsequently observed. We now need to make the correspondence among the points plotted in Fig. 2 to "actionable information", i.e., how the relative positions of the satellites have changed between two sets of observations.

Now let us assume that the observations are repeated on a later night, with the objects again distinguished (sorted) by the same convention (e.g., longitude then latitude). This time, the observed ratios for the configuration assume a different value in Fig. 2; let's say the uppermost point (2.0/1.4, 2.8/1.4). Comparing these "before" (circled point) and "after" (uppermost point, labeled 3 on the figure) ordered pairs shows that the three objects have been cyclically permutated: Object 1 has assumed Object 3's position, whereas Object 3 has moved to Object 2's position and Object 2 has moved to Object 1's position – the S3 permutation is denoted (231).

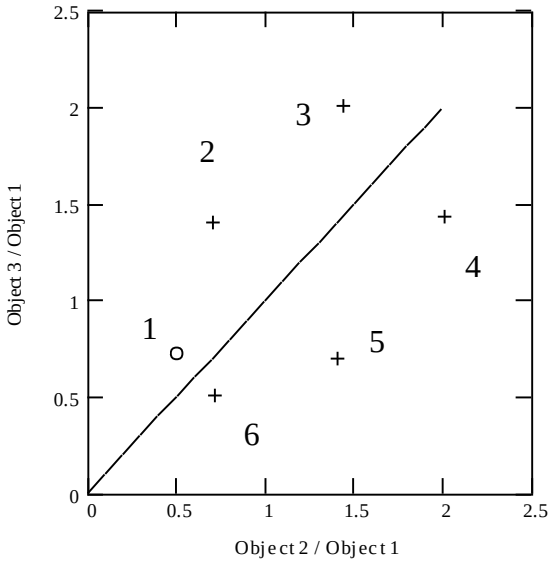

Fig. 2. The six values of the ordered pairs of ratios (phase curve curvature; see text) corresponding to the six object configurations of a three-object cluster.

Paper I shows how to calculate the "transition permutation" (P_t) from an initial (i) configuration to a final (f) configuration, $P_t = P_f * P_i^{-1}$, where P_i^{-1} is the inverse of the initial configuration (represented as a permutation), and P_f is the final configuration. In the example above, P_i is the identity corresponding to the original configuration, P_i^{-1} is also just the identity, and the transition permutation, $P_t = P_f = (231)$, is the cyclical permutation of the three objects that was found above.

As a second example, now consider (12) as the new starting configuration (corresponding to the rank-ordering of the Table 1 objects by longitude and latitude in the order GOES 10, Anik F1, and "Synthetic"), so the first observation of the configuration on the first night is Point 4 on Fig. 2 (the rightmost point). If the next night's observed ratio pair turns out to be Point 5 (middle of three points below the line), the job of the person interpreting the two observations is to determine how the configuration changed. Once again using $P_t = P_f * P_i^{-1}$, with $P_i = (12)$, $P_i^{-1} = (12)$, and $P_f = (312)$, the transition permutation is found to be (13), so that Objects 1 and 3 (GOES 10 and "synthetic") have exchanged places. This can be verified by looking at the decomposition of the ratios in Table 2. The reader will note that the transition permutation is independent of which of the six points in Fig. 2 is chosen as the identity configuration. For example, the uppermost point in the figure could be defined as the identity, and the points proceeding clockwise from it would be (23), (231), (13), (312), and (12). Although the initial and final permutations that define the configurations differ with a change in definition of the identity, the calculated transition permutations are equal, as they should be for a given change in object configuration.

The extension of Paper I's technique to phase curves proves to be a powerful technique. First, Paper I's spectral data can be collected nearly simultaneously for objects that reside in the same slot in the geo-belt;

changing atmospheric transmission has a minimal impact in this case. By contrast, phase curve data necessarily requires waiting for objects to revolve with the Earth's rotation to achieve the range of desired phase angles; atmospheric transmission has a greater likelihood of changing over the course of the night. Nevertheless, each of the points on Fig. 2 is independent of atmospheric transmission changes over the longer time intervals between phase angle samples, since each point involves ratios of signal pairs acquired at the same phase angle, and attenuated equally (to a good approximation) by the Earth's atmosphere. Secondly, phase curves may have desirable characteristics over individual object spectra, since the phase curve is sensitive over the range of satellite structures that are preferentially illuminated by different phase angles[4]. For this reason, an individual object's spectrum may have a phase angle dependence that limits use of the spectrum as a means of identification to specific phase angles. Both techniques should be evaluated for a sample of objects to determine their individual strengths and weaknesses.

3. THE SBIR EFFORTS

The four efforts under SBIR Topic AF093-056 fall into two groupings, with two efforts focusing on spectral approaches (with a grating or prism as the dispersive element), and two being multi-waveband in nature. The spectral approaches are exploring innovative concepts for acquiring all spectral data simultaneously; one has the capability to obtain spectra of multiple objects falling in an acquisition camera's field of view in the same time interval, whereas the other approach employs a high sensitivity, electron-multiplication CCD in order to minimize integration time, achieve adequate spectral SNR on typically one object at a time, and thereby maximize the number of objects observed during the night.

The multi-waveband approaches emphasize a small number of carefully selected spectral filter bands to fully distinguish the geosynchronous object on the basis of their multi-band signals. One of these approaches exploits the existing photometric channels of GEODSS (the 32x32 pixel Photometers A or B), by enhancing the sensor array with a 2x2 square filter pattern onto which the image of the geosynchronous satellite can be steered by telescope pointing, successively acquiring the 4 multiband measurements. This approach clearly provides a "minimal impact upgrade" to GEODSS to multi-spectral capability. The other approach uses clever optical element design to segregate the image of an object into multiple colors that appear over different sectors of a single, large sensor array. The simultaneous nature of the multiband data acquisition permits interesting color reconstructions and provides a certain amount of atmospheric turbulence compensation for non-geosynchronous objects subtending angles on the scale of the atmospheric seeing limit.

This paper benefited from helpful discussions with Drs. Anil Chaudhary and Tamara Payne. Acknowledgment is given for original SBIR topic guidance to ESC/XR, Darin Leahy & Harvey Tobin.

4. REFERENCES

1 Scott, R.L. & Wallace, B., Small Aperture Telescope Observations of Co-located Geostationary Satellites, 2009 AMOS Technical Conference Proceedings.

2 LeVan, P., Closely-spaced objects and mathematical groups combined with a robust observational method, 2009 AMOS Technical Conference Proceedings ("Paper I").

3 Payne, T.E., Gregory, S.A., Villafuerte, J., The development of a satellite signatures testbed based on the Raven system, Proc. of SPIE, Vol. 5489, doi: 10.1117/12.551835, 2004.

4 Payne, T.E, Chaudhary, A., Gregory, S.A.,, Brown, J., and Nosek, M., Signature intensity derivative and its application to resident space object typing, 2009 AMOS Technical Conference Proceedings.